A-23

PLASTIC SHEAR FLOW IN ASYMMETRICALLY NOTCHED SPECIMENS

A. Guillén-Preckler [×]
F. A. McClintock [××]
R. D. White [×××]

ABSTRACT

Ductile fracture depends upon the history of stress and strain, and also upon the rotation of material elements relative to axes of stress and strain. Asymmetrically notched specimens are proposed for which those quantities can be theoretically found for incompressible plastic flow under plane strain conditions. The theoretical predictions are then compared to the experimental results and the important role of the strain hardening is shown.

[×] "Profesor del Departamento de Mecánica". E.T.S.I.I. University of Navarra (Spain).

[××] Professor of Mechanical Engineering. Massachusetts Institute of Technology (U.S.A.).

[×××] Formerly at the Mechanical Engineering Department of M.I.T. (U.S.A.).

PLASTIC SHEAR FLOW IN ASYMMETRICALLY NOTCHED SPECIMENS

INTRODUCTION

Ductile fracture, particularly by the growth of voids, depends upon the history of stress and strain, and also upon the rotation of material elements relative to axes of stress and strain. Experiments to determine fracture characteristics should be carried out on specimens for which these factors are known.

The stress distribution in grooved specimens gives little trouble, although in relatively few cases have the grooves been deep enough to prevent yielding in the shoulders. For a summary of the required depth of groove for various shapes, see McClintock[1].

The importance of strain can be shown by holding the stress distribution constant using specimens with grooves of unequal angles. For a non-hardening material, this confines displacements to the zones of Fig. 1, and gives a strain infinity at the point **p**. Actually, strain hardening spreads the deformation outside the bands (McClintock and Rhee)[2] so the strain is indetermined, from usual slip line theory. Even so, the unequal groove angles tend to concentrate the strain, and a reduction in fracture load has been reported by McClintock[1].

The strain distribution is more nearly known for the symmetrical, doubly-grooved, plane-strain specimen of non-hardening rigid-plastic material. Lee and Wang[3] developed the deformation for the limited flow field of Hill[4], which has a singularity where two fields Join, similar to that of Fig. 1. Neimark[5] applied the extremum theorems of Hill[6] to show that the displacements should vary linearly, rather than being uniform. in the central zone between the two regions of logarithmic spirals extending from the notch root. Rosenfeld[7] corroborated this result, but also showed that it did not give a completely

correct solution along the slip lines which formed the boundary of the fully plastic field. Apparently this is because the rapid growth of the plastic zone for a strain-hardening material admits solutions that are not to be found among the admissible displacement fields for a non-hardening material.

To eliminate at least one pair of the troublesome slip lines, the antisymmetric specimen shown in Fig. 2 is proposed. The flow is primarily shear with a concurrent rotation in the S shaped band ACQPB'A'SRB. The triaxial stress is set by the flank angle. The specimen may thus simulate the shear zones often encountered in metal processing.

ANALYSIS AND THEORETICAL RESULTS

The material is assumed to be rigid-plastic and under conditions of plane strain. The slip line field used here is the one given by A.P. Green[8] for a strong junction with wedge-shaped sides and finite root radius, and it is shown in Fig.2.

The stresses in the plastically deforming region can be found by means of the Hencky equations and Mohr circles, since we have plane strain conditions.

Hencky equations in the customary form are

$p + 2K\Phi = \text{const.}$, along α lines

$p - 2K\Phi = \text{const.}$, along β lines

Where

$$p = -\frac{\sigma_1 + \sigma_2 + \sigma_3}{3} = \text{-triaxial stress}$$

$\sigma_1, \sigma_2, \sigma_3$ principal stresses

Φ counterclockwise angle from the+ x direction to the+ αdirection at any point.

The Mohr circles at the regions 1 (flank) and 2 (core) are the ones given in Fig. 3.

Table I and Fig. 4 give a summary of the stresses obtained by integrating the Hencky equations along the slip lines.

Table I

stress	at root of grove	in core
σ_1	$2k$	$k(\pi+2-2\theta)$
σ_2	0	$k(\pi-2\theta)$
$\sigma/\bar{\sigma} = \frac{\sigma_1+\sigma_2+\sigma_3}{3\sqrt{3}k}$	$1/\sqrt{3}$	$(\pi+1-2\theta)/\sqrt{3}$

where

$$\sigma = -p$$
$$\bar{\sigma} = k\sqrt{3}, \text{ equivalent stress}$$

The dimension of the core region of uniform strain and stress, s= QR in Fig. 2, is related to the minimum thickness (b) and the root radius (a) by the purely geometrical relationship

$$s = \sqrt{2}\left[(b/2)+a(1-e^{-\theta+\frac{\pi}{2}})\right] \qquad (1)$$

As the specimen deforms, the new shape can be approximated by new values of quantities in Eq. 1, as was done by Wang[9] in studying the symmetrically grooved specimens. To obtain the displacements the Geiringer equations were integrated numerically over a 5° mesh (White[10], see Appendix). Along lines of maximum and minimum shear stress, respectively, these equations are

$$du - v\,d\phi = 0 \qquad (2)$$
$$dv - u\,d\phi = 0$$

The relation between the axial specimen elongation (δL) and the displacement (δV)

$$(\delta L) = (\delta V)\sqrt{2}$$

And now the following relationships can be written

$$\frac{\delta(a/a_o)}{\delta(L/a_o)} = \frac{\delta a}{\delta V}\frac{1}{\sqrt{2}} \quad ; \quad \frac{\delta(b/b_o)}{\delta(L/a_o)} = \frac{\delta b}{\delta V}\frac{1}{\sqrt{2}}$$
$$\frac{\delta(Y_c/a_o)}{\delta(L/a_o)} = \frac{\delta Y_c}{\delta V}\frac{1}{\sqrt{2}} \quad ; \quad s = \sqrt{2}\left[(b/2)+a(1-e^{-\theta+\frac{\pi}{2}})\right] \qquad (3)$$
$$\frac{\delta(S/S_o)}{\delta(L/a_o)} = \frac{(b_o/S_o)\,\delta(S/b_o)}{\delta(L/a_o)} = \frac{b_o}{S_o}\,\frac{\sqrt{2}\left[\delta(b/b_o)/2 - \delta(a/b_o)(e^{-\theta+\frac{\pi}{2}})\right]}{\delta(L/a_o)}$$

Chatwin[11], by assuming constant tangency of flank angle and root circle, found graphically the values of ($\delta a/\delta V$), ($\delta b/\delta V$), and ($\delta Y_c/\delta V$) for different flank angles, Figs. 5 and 6, and he found also that those incremental ratios were only slightly dependent on the geometry of the specimen (say on s/a) as compared to their dependance on the current flank angle, he observed that the centers of curvature of the root circle stayed very nearly opposite to each other. In symbolic form, if Y_c denotes the Y coordinate of the approximate center of curvature of the notch,

$$\frac{\delta Y_c}{\delta L} < 0.1\,\frac{\delta b}{\delta L}$$

Furthermore the rates of shape change given by Figs. 5 and 6 depended primarily on the root radius and were nearly independent of the band width. Therefore the curves of Figs. 5 and 6 could be used not only for the original, but also for the current values.

It can be shown also that for small (δV)

$$\frac{\delta\theta}{\delta V} = -\frac{1}{S}$$

and therefore

$$\frac{\delta\theta}{\delta(L/a_o)} = -\frac{1}{\sqrt{2}}\left[\frac{1}{(S/a_o)}\right] = -\frac{1}{\sqrt{2}}\,\frac{a_o}{S_o}\,\frac{1}{S/S_o} \qquad (4)$$

Finally knowing already the current values of

$(\delta a/\delta\gamma)$, $(\delta b/\delta\gamma)$ and $(\delta Y_c/\delta\gamma)$, and using them in formulas (3) and (4) one obtains the quantities $\delta(a/a_o)$, $\delta(b/b_o)$, $\delta(Y_c/a_o)$, $\delta(s/s_o)$, $\delta\theta$ and from them the current values of (a), (b), (Y_c), (s), and θ during the deformation.

Based on Eqs. 3 and 4 a computer program was written which by using Chatwin's results gave the integrated values of the ratios (a/a_o), (b/b_o), (Y_c/a_o), (s/s_o).

The magnitude of the step of integration used by the computer was the smaller of the two values $\delta\theta = 0.5°$ or $(\delta \frac{a}{a_o}) = 0.05$, at any moment.

The results of the numerical integration are presented in Figs. 7 and 8, for the shapes tested. Further results are presented in Guillén Preckler[12].

It is of interested at this point to notice that the current strains at the root and at the core can be obtained.

The expression for the strain increments at points located on the root circle is somewhat involved (see reference 12, p. 16), but the expression for the strain increments at the core is a rather simple one

$$\frac{\delta\gamma}{\delta L/a} = \sqrt{2}/k_1, \text{ where } k_1 = s/a$$

The equivalent relative strain increments in the root at the critical points B and D, are given for various flank angles in Fig. 9. The equivalent relative strain increments at the core as a function of the relative root sharpness are given in Fig. 10.

SELECTION OF SPECIMENS

In actual materials, strain hardening in the deforming region tends to spread out the zone of plastic deformation, thus reducing the strain for given specimen extension. It is therefore desirable to choose a specimen such that widening of the plastic

band due to strain hardening will involve the largest possible increase in the length of slip lines which have to deform plastically.

To maximize the rigidity of the material beyond the plastic band in this way and thus to minimize the effect of strain hardening, it is desirable to choose specimens with sharp notches (s/a large) and small flank angles.

On the other hand, to study the effects of triaxiality on fracture behaviour, it is necessary to have the crack initiate in the core rather than at the root. The strain increments at the root, shown in Fig. 9, are independent of (a/s), while those in the diamond-shaped core increase with (a/s) as shown in Fig. 10. Therefore to increase the likelihood of fracture at the core the value (a/s) should be maximized. The likelihood of core fracture is greater the smaller the flank angle. Thus both strain hardening and fracture considerations suggest a small flank angle, but to obtain sufficient ductility for the fully plastic analysis to have meaning, the value cannot be too small.

The first compromise between the above factors was chosen to be

$$\theta = 45°, \qquad a_o/b_o = 0.0925$$

which gave a satisfactory extension for specimens of Al 6061-T6 tested under a pressure of 68,000 psi, whereas

$$\theta = 60°, \qquad a_o/b_o = 0.125$$

was necessary for reasonable ductility of Al 7075-0 at room pressure.

More recently another experimental technique to measure the current shape of the notch profile has been developed; essentially it is based on using dental synthetic rubber to obtain replicas of the notch of the specimen.

This technique has been used in testing one 60° flank angle with (a_o/b_o) = o.125, and one 45° flank angle with (a_o/b_o)= 0.0925 specimens, at room pressure; the material for both those specimens was EARSIMAG-10 TM.

EXPERIMENTAL RESULTS

The test run at atmospheric pressure on the 45° flank angle specimen (Al 6061-T6) gave too small deformation to be accurately measured; for that reason a tension test under hydrostatic pressure (68,000 psi) was run on a similar specimen. The data from the test are shown in Fig. 8, in this case the total specimen extension was so large that the theory would predict a negative value for the band width (s) (see Fig.7)

One 60° flank angle specimen (Al 7075-0) was tested at room pressure, the results are also given in Fig.8 The shape changes, compared to the theory were in this case

$$(\delta\theta)_{test} = 44 \text{ percent of } (\delta\theta)_{theory}$$
$$(\delta\frac{a}{a_o})_{test} = 100 \text{ " " } (\delta\frac{a}{a_o})_{theory}$$
$$(\delta\frac{b}{b_o})_{test} = 61 \text{ " " } (\delta\frac{b}{b_o})_{theory}$$

The last tests run on the 60° and 45° flank angle specimens of EARSIMAG-10 TM at room pressure gave the results labelled with triangles in Fig. 8, those results compared to the theory give for the 45° flank angle specimen,

$$(\delta\theta)_{test} = 95.4 \text{ percent of } (\delta\theta)_{theory}$$
$$(\delta\frac{a}{a_o})_{test} = 91.6 \text{ " " } (\delta\frac{a}{a_o})_{theory}$$
$$(\delta\frac{b}{b_o})_{test} = 105.4 \text{ " " } (\delta\frac{b}{b_o})_{theory}$$

for the 60° flank angle specimen

$$(\delta\theta)_{test} = 67 \text{ percent of } (\delta\theta)_{theory}$$
$$(\delta\frac{a}{a_o})_{test} = 106.2 \text{ " " } (\delta\frac{a}{a_o})_{theory}$$
$$(\delta\frac{b}{b_o})_{test} = 84.1 \text{ " " } (\delta\frac{b}{b_o})_{theory}$$

CONCLUSIONS

A theoretical analysis based on the assumption of no strain hardening provides the stress and strain histories in a shear band in an asymmetrically grooved specimen. The experimental discrepancy indicates that strain hardening in the aluminun alloys 6061 and 7075 is large enough to make the results of limited value in cuantitative studies of the history of stress and strain before fracture. The experimental results obtained from EARSIMAG-10 TM specimens are the closest to the theoretical predictions, this corroborates the previous conclusion since this material has very low strain hardening characteristics.

ACKNOWLEDGMENT

The authors deeply appreciate the support of part of this work by I.I.E. and by the National Science Foundation through Grant G-14995. The assistance of Mr. Ray Landis and Terry Chatwin in carrying out numerical calculations, and of Mr. Elias Goñi in the experimental work must also be acknowledged. Finally we wish to mention the invaluable help of Mr. Stuart Madnick in the computer work done through the courtesy of the Computation Centers of M.I.T. and of E.T.S.I.I. (University of NAVARRA)

NOTE ON MATERIAL PROPERTIES;

Alloy	6061	7075	EARSIMAG-10
Silicon	0.4-0.8	0.5	0.6-1.3
Iron	0.7	0.7	0.6
Copper	0.15-0.4	1.2-2.0	0.15
Manganese	0.15	0.3	0.45 -1.0
Magnesium	0.8-1.2	2.1-2.9	0.45 -1.0
Chromium	0.15-0.35	0.18-0.4	....
Nickel	....	....	....
Zinc	0.25	5.1-6.1	0.1
Titanium	0.15	0.2	....
Aluminum	rest	rest	rest

REFERENCES

1) F.A. McClintock, Welding Jnl. Res. Suppl. 26, 202 (1961).
2) F.A. McClintock and S.S. Rhee, Proc. 4th Nat. Congress of Appl. Mech., 1007 (1962)
3) E.H. Lee and A.J. Wang, Proc. 2nd Nat. Congress of Appl. Mech., 489 (1954).
4) R. Hill, Rhe Mathematical Theory of Plasticity, Oxford University Press, Oxford, England, 129 (1950).
5) J.E. Neimark, Sc. D. Thesis, Mech Eng. Dept., M.I.T. (1959).
6) R. Hill, Jnl. Mech. and Physics of Solids, 4, 247 (1956).
7) R.L. Rosenfeld, Res. Mem. No. 20, Fatigue and Plasticity Lab., Dept. of Mech. Eng., M.I.T. (1959).
8) A.P. Green, Jnl. Mech. and Physics of Solids, 2, 197 (1954)
9) A.J. Wang, Quart. of App. Math., 11, 427 (1954).
10) R.D. White, B.S. Thesis, Mech. Eng. Dept., M.I.T. (1961)
11) T. Chatwin, Res. Mem. No. 50, Fatigue and Plasticity Lab., Dept. of Mech. Eng., M.I.T. (1963)
12) A. Guillén Preckler, M.S. Thesis, Mech. Eng. Dept., M.I.T. (1964)

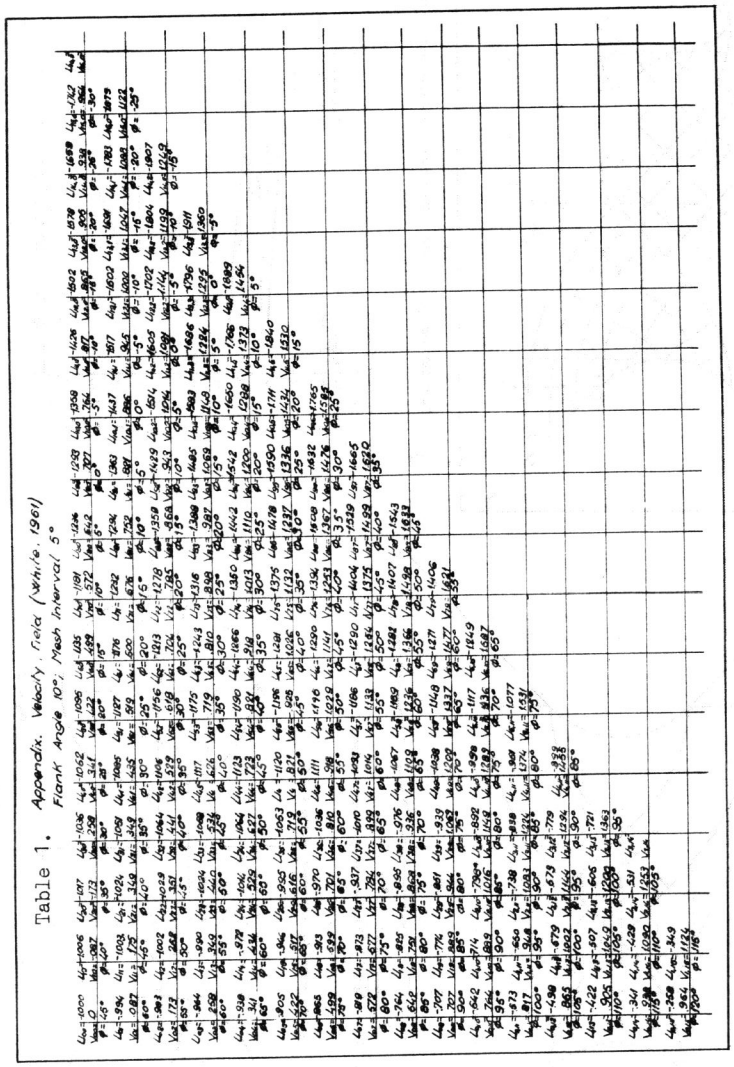

Table 1. Appendix. Velocity Field (White, 1961)
Flank Angle 10°, Mesh Interval 5°

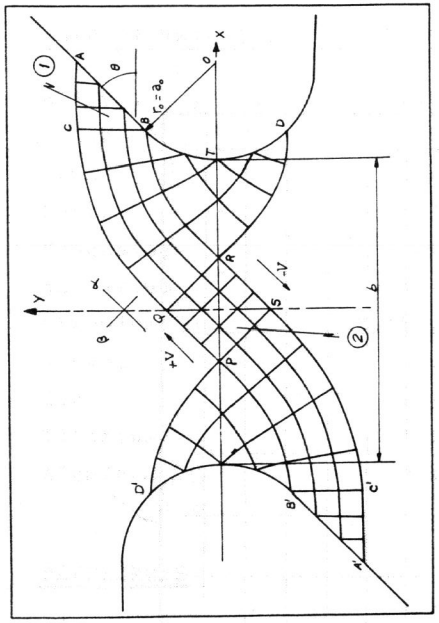

Fig 2- Geometry of the specimen and slip-line field

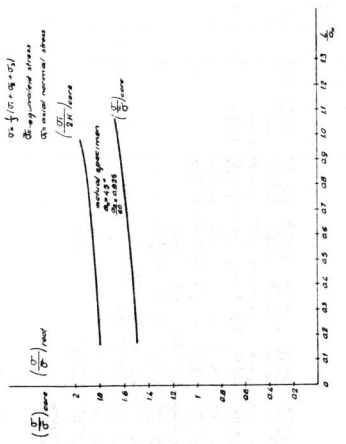

Fig 4- Stress ratios at the root and at the bars vs extension

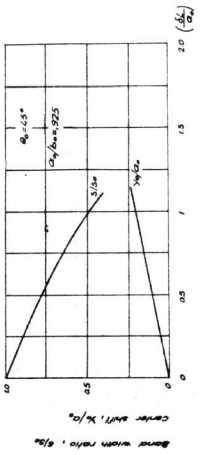

Fig 7- Decrease in band width and shift of center of curvature due to extension.

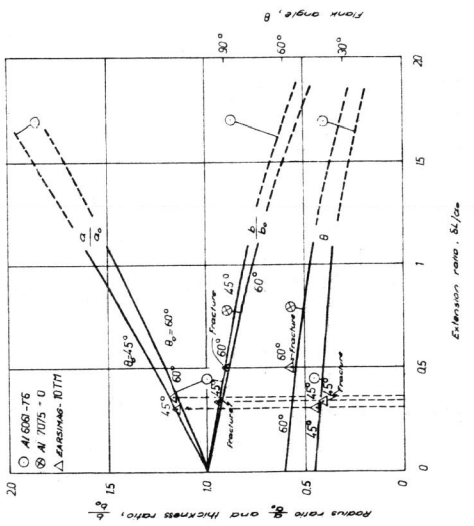

Fig 8- Blunting and deepening of groove and decrease of flank angle, as a function of extension. Note:
For θ_0=45° ; a_0/b_0 chosen 0.925
60° ; a_0/b_0 chosen 1.25

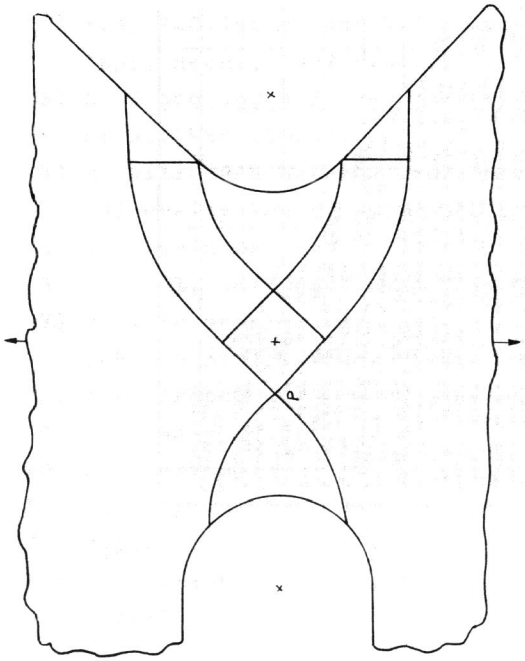

Fig 1- Plastic flow field for unequal groove angles.

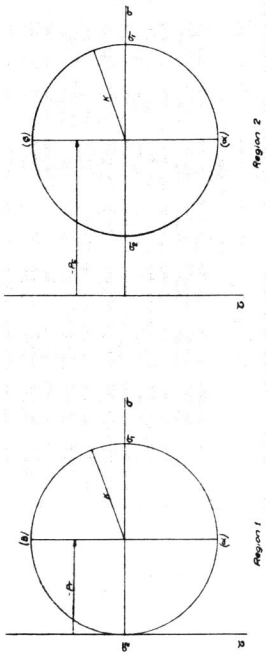

Fig 3- Mohr Circles.

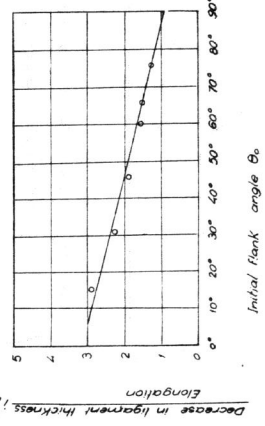

Fig 5- Rate of decrease of ligament thickness b with elongation

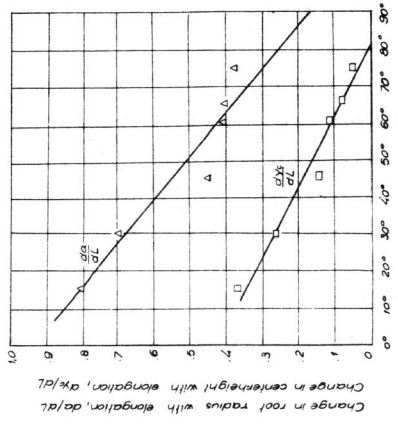

Fig 6- Change in radius and y coordinate of centerof root with elongation

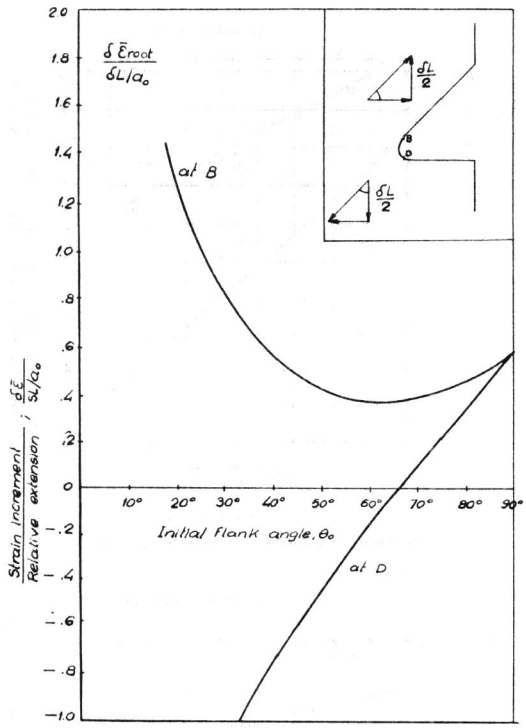

Fig. 9.- Strain increments at B and D as a function of initial flank angle (independent of a_0/ℓ_0).

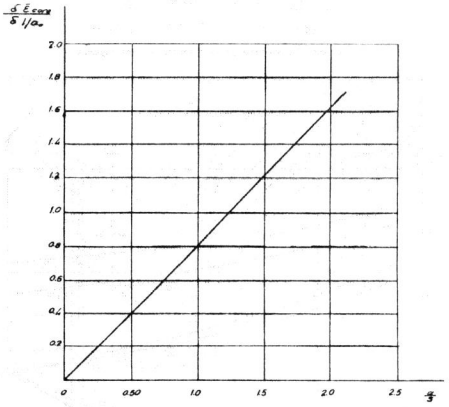

Fig 10.- Strain increments in the core as a function of relative root sharpness.

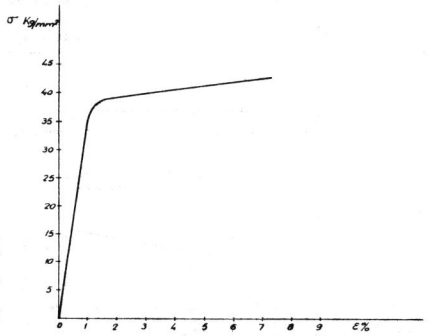

Fig 11.- Earsimag-10 T.M. True Stress-Strain diagram